SHEAR WAVE VELOCITY TO EVALUATE IN-SITU STATE OF OTTAWA SAND

by

P.K. Robertson [1], M.ASCE, S. Sasitharan [2],

J.C. Cunning[1], and D.C. Sego [1], M.ASCE

[1] Geotechnical Group
Department of Civil Engineering
University of Alberta
Edmonton, Alberta, Canada
T6G 2G7
Tel: (403) 492-5106
Fax: (403) 492-8198

[2] Powertech Lab Inc.
12388 - 88 Avenue
Surrey, B.C., Canada
V3W 7R7
Tel. (604) 590 - 7500
Fax: (604) 590 - 5347

Submitted to

Journal of Geotechnical Engineering

American Society of Civil Engineering

May, 1994

Abstract

The initial state of a sand, defined by the void ratio and effective mean normal stress, can be used to predict its large strain response. Laboratory studies have shown that the shear wave velocity of a sand is controlled primarily by the effective confining stresses and void ratio. Since the shear wave velocity can be measured both in the field and in the laboratory, there is increasing interest in using shear wave velocity to define the state of a sand. This paper presents an experimental study of shear wave velocity interpretation for clean Ottawa sand based on steady/critical state concepts. Results presented show that the large strain behavior of Ottawa sand can be estimated using shear wave velocity measurements combined with a knowledge of the *in-situ* effective stress. Based on a knowledge of the state of a sand, it is possible to identify the boundary between either a contractant or dilatant sand at large strains. Based on these findings, a preliminary method to evaluate the potential for flow liquefaction using shear wave velocity measurements is presented.

Key words: Shear wave velocity, sands, state parameter, liquefaction, laboratory testing.

INTRODUCTION

Roscoe *et al.* (1958) and Been and Jefferies (1985) showed that the large strain behavior of a soil can be expressed in terms of the initial state relative to the steady/critical state at the same stress level. Soils with an initial state above the steady/critical state undergo a net contraction when sheared to critical state. If the initial state of a soil lies below the critical state then a net dilation occurs when sheared to critical state. Therefore, the initial state defined by the void ratio and mean normal stress, can be used to identify the large strain behavior.

"Dense" sands tend to dilate during shear at large strains and hence generally provide excellent stability under most loading conditions. However, "loose" sands can contract during shear at large strains. During undrained shear, loose sands can develop large pore pressures and can strain soften. Hence, it can be important to identify, using in-situ testing, the boundary between "loose" and "dense" sands.

During monotonic undrained loading, a loose sand can reach a peak resistance and then rapidly strain soften to a constant resistance at which the effective stress state remains constant. Castro (1969) termed this ultimate constant state as the steady state and showed that it represents a state in the void ratio (e)-effective mean normal stress (p')-deviator stress (q) space. If the in-situ shear stresses are larger than the ultimate strength at steady state, large flow deformations can occur. Castro (1969) defined this flow deformation as liquefaction. Been *et al.* (1991) showed that the ultimate steady state achieved during monotonic undrained loading is also a critical state implying that steady state is independent of the stress path followed; i.e., ultimate steady state is unique for a void ratio regardless of whether it was reached via drained or undrained loading.

In practice, the generic term liquefaction is used to describe different mechanisms. Seed *et al.* (1983), using the results of extensive cyclic triaxial testing, defined

liquefaction as the condition of zero effective confining stress due to cyclic loading with shear stress reversal. At zero effective stress, a cohesionless soil has very little stiffness and large deformations can develop during cyclic loading. In Japan, it is common to define liquefaction in terms of the magnitude of the cyclic stress ratio required to produce a given level of strain, typically 5% double amplitude axial strain (Ishihara, 1993). Robertson (1993) suggested that liquefaction should be defined as either flow liquefaction or cyclic liquefaction. Flow liquefaction closely follows the definition of liquefaction suggested by Castro (1969). Flow liquefaction requires a strain softening response in undrained shear loading and *in-situ* gravitational shear stresses greater than the ultimate critical/steady state strength. Liquefaction from cyclic loading can be further subdivided into either cyclic liquefaction or cyclic mobility. Cyclic liquefaction occurs during undrained cyclic loading where shear stress reversal or zero shear stress can develop (i.e., where the *in-situ* gravitational shear stress is low compared to the cyclic shear stress). Cyclic liquefaction also requires that sufficient undrained cyclic loading occurs to allow the effective confining stress to essentially reach zero. At zero effective confining stress, the soil has very little stiffness and large deformations can result even under very small gravitational shear stresses. Cyclic mobility results when there is no shear stress reversal during undrained cyclic loading. Hence, the condition of zero effective stress does not develop and deformations tend to be smaller and eventually stabilize.

The first step when evaluating liquefaction potential (flow liquefaction, cyclic liquefaction and cyclic mobility) is to evaluate the *in-situ* state of the soil and hence the material characteristics in terms of strain softening or strain hardening responses (Robertson, 1993). If the soil is strain softening, flow liquefaction is possible if the soil can be triggered to collapse and if the gravitational shear stresses are larger than the ultimate steady state or residual strength. The trigger to cause collapse can be either monotonic or cyclic. Whether a slope or soil structure will slide or flow depends on the

amount of strain softening soil relative to the strain hardening soil within the structure and the brittleness of the strain softening soil. If the soil is strain hardening, flow liquefaction will not occur unless pore pressure redistribution resulting from cyclic loading causes the soil to change void ratio. However, cyclic liquefaction or cyclic mobility can still occur due to cyclic (seismic) undrained loading.

One preferred method to evaluate the *in-situ* state of the soil and hence the response of a soil to a given loading is to obtain high quality undisturbed samples and perform laboratory testing following the appropriate stress path. However, this process is difficult in cohesionless soils such as sand. *In-situ* ground freezing has recently been used to successfully obtain high quality undisturbed samples of cohesionless soil (Yoshimi *et al.*, 1984; Hatanaka *et al.*, 1985; Yoshimi *et al.*, 1989; Sego *et al.*, 1993). However, the cost of *in-situ* ground freezing is high and is currently restricted to larger projects. For small projects and in the initial investigative stages of large projects, *in-situ* testing such as the Standard Penetration Test (SPT) and the Cone Penetration Test (CPT) have been the most commonly used approaches to evaluate *in-situ* state and hence, liquefaction potential. Most of the existing methods to evaluate liquefaction potential from these *in-situ* tests are applicable to cyclic liquefaction and are based on the cyclic stress ratio to trigger a given level of deformation (either cyclic liquefaction or cyclic mobility). Most methods are for level ground conditions and corrections are required for sloping ground (Seed *et al.*, 1983). In general, these methods have proven to be very good at predicting cyclic liquefaction for essentially level ground conditions (Kayen *et al.*, 1992). However, their application to predict the trigger of flow liquefaction in very loose sands for steeply sloping ground is uncertain. Robertson *et al.* (1992a) and Ishihara (1993) have suggested a range of values for penetration resistance from the SPT and CPT to evaluate if a strain softening response and hence, the potential for flow liquefaction, is possible. Sladen and Hewitt (1989) also suggested a profile of CPT based on back analysis of several flow liquefaction failures of hydraulically placed sand used for construction of artificial islands

in the Beaufort sea. Robertson *et al.* (1992a) suggested values for shear wave velocity normalized with respect to vertical effective stress to evaluate the *in-situ* state of cohesionless soils.

This paper presents results from an experimental study to evaluate whether shear wave velocity (V_S) can be used to identify the *in-situ* state of a given sand relative to the critical/steady state. Based on knowledge of the *in-situ* state of a sand it should be possible to then estimate the large strain behavior of the sand in terms of contractant (strain softening) response or dilatant (strain hardening) response to undrained shear.

PREVIOUS WORK ON SHEAR WAVE VELOCITY

The shear wave velocity is controlled primarily by the void ratio, the effective confining stresses, the intrinsic characteristics of the soil (grain size distribution, grain shape, angularity, surface roughness and mineralogical composition) and the structure (fabric, interparticle forces and bonds). Unless significant grain crushing occurs, the intrinsic characteristics of the soil do not change with changes in void ratio and effective confining stresses, although the structure can change somewhat. Despite this, in many uncemented cohesionless soils, shear wave velocity can be regarded as a fundamental parameter. Hence, there is increasing interest in using shear wave velocity to define the state (void ratio, and effective confining stresses) of a soil, since shear wave velocity can be measured both in the field and in the laboratory.

Based on resonant column test results, Hardin and Richart (1963) found that the small strain shear modulus (G_0) and hence shear wave velocity can be related to effective mean normal stress and void ratio by:

$$V_S = (m_1 - m_2 e)\,(p')^{0.25} \qquad (1)$$

where: V_s = shear wave velocity;

e = void ratio;

p' = effective mean normal stress;

m_1 and m_2 = material constants.

Hardin and Richart (1963) further suggested that m_1 and m_2 have values of approximately 111 and 51 when stress is measured in kPa and shear wave velocity is measured in m/s. However, the Hardin and Richart (opt. cit.) equation was based on observations made on isotropically consolidated sand. An alternative equation, was proposed by Roseler (1979) based on tests with cubic specimens where stresses can be applied independently. His results suggested that individual stresses play an important role on the wave travel rather than the mean normal stress as proposed by Hardin and Richart (1963). Hence, Roseler proposed that:

$$V_s = (m_1 - m_2 e)\,(\sigma'_a)^{na}\,(\sigma'_p)^{nb} \qquad (2)$$

$$V_s = (A - Be)\left(\frac{\sigma'_a}{P_a}\right)^{na}\left(\frac{\sigma'_p}{P_a}\right)^{nb} \qquad (3)$$

where $A = m_1 (P_a)^{na + nb}$

$B = m_2 (P_a)^{nb + nb}$

$na = nb = 0.125$, typically.

Yu and Richart (1984) and Stokoe *et al.* (1985) showed that the exponents na, nb were equal with a value of about 0.125. Further, for dense sands, de Alba *et al.* (1984) found that shear wave velocity is also slightly influenced by the soil fabric created using different sample preparation methods. Here soil fabric refers to the micro structure of the sand that involves the orientation and the distribution of contacts between grains.

There have been several attempts in the past to correlate cyclic liquefaction resistance to shear wave velocity (Bierschwale and Stokoe, 1984; Tokimatsu *et al.*, 1986;

Tokimatsu and Uchida, 1990; Robertson *et al.*, 1992a and 1992b). Robertson *et al.* (1992a) used a normalized shear wave velocity given by:

$$V_{s1} = V_s\left(\frac{P_a}{\sigma'_v}\right)^{0.25} \qquad (4)$$

where: V_{s1} = the normalized shear wave velocity;

V_s = the shear wave velocity;

P_a = the reference pressure (usually 100 kPa);

σ'_v = the effective overburden pressure.

Based on CPT and field shear wave velocity measurements, Robertson *et al.* (1992a) suggested a critical value of V_{s1} between 140 and 160 m/s that separates a contractive strain softening response from a dilative strain hardening response at large strains in clean sand. However, evaluation of this critical value was limited to one site and did not fully incorporate the steady state concept.

Equation (4) assumes that the coefficient of each pressure at rest (K_o) is equal to unity. Hence, Equation (4) should be modified as follows;

$$V_{s1} = V_s\left(\frac{P_a}{\sigma'_v}\right)^{0.25}\left(\frac{1}{K_o}\right)^{0.125} \qquad (5)$$

However, for most reasonable values of K_o for loose sand ($0.4 < K_o < 1.0$) equation (4) is within 12% of equation (5).

TESTING PROGRAM

A modified Wykeham Farrance triaxial test apparatus described by Sasitharan *et al.* (1993) was used throughout this study. Shear wave velocities were generated and received using bender elements (Shirley, 1978) in the triaxial specimen. The bender

elements, consisting of two thin plates of ceramic material rigidly bonded together, were installed at the top and bottom pedestal of the triaxial cell. Details are described by Sasitharan *et al.* (1994a). The polarization of the ceramic material in each bender element and the electrical connection is such that when a driving voltage is applied to the bender element, one plate elongates and the other shortens. One edge of the bender element protrudes into the specimen as a cantilever. The surrounding soil particles move in the same direction as the tip of the bender element. This generates a shear wave that propagates vertically through the sample.

The bender element can also be used as a receiver. When the shear distortion reaches the receiving bender element embedded in the specimen it creates a mechanical vibration, which causes one layer of the bender element to undergo extension while the other undergoes compression, hence, generating an electrical pulse that is displayed on the oscilloscope screen. The travel time of the shear wave through the specimen is determined from the time lag of the pulse reaching the receiving bender element. Hence the shear wave velocity is determined from the travel time and length of travel.

A schematic layout of the shear wave velocity measuring system in the triaxial apparatus is shown in Figure 1. Using this measuring system, the change in shear wave velocities during consolidation and triaxial loading can be investigated for a given specimen.

Ottawa (C 109) sand obtained from Ottawa, Illinois was used in this study. Ottawa sand is a uniform sand with a mean grain size (D_{50}) of 0.35 mm and is comprised primarily of quartz with a specific gravity of 2.67. The maximum and minimum void ratios of the sand determined using the ASTM method D2049 are 0.82 and 0.50, respectively.

Uniform Ottawa sand specimens were prepared using the water pluviation (WP) technique described by Negussey (1984) and Sasitharan (1989). However, it was observed that very loose sand specimens could not be prepared by water pluviation. This is consistent with the observation made by various other researchers regarding water pluviated sand specimens (e.g., Han and Vardoulakis, 1991). Hence, very loose uniform sand specimens were also prepared using the moist tamping (MT) technique described by Sasitharan *et al.* (1993).

Ottawa sand specimens prepared very loose (e = 0.89 - 0.80), medium dense (e = 0.66 - 0.68) and dense (e = 0.57 - 0.59) were initially consolidated to an isotropic consolidation stress of 50 kPa. Then the specimens were isotropically consolidated by 50 or 100 kPa stress increments depending on the final consolidation stress. During consolidation, dead loads were added to the top of the specimen to compensate for the uplift force acting on the loading ram. This ensured that the specimens were consolidated isotropically and that the bender element maintained contact. After applying a stress increment, the specimen was allowed to fully consolidate. For Ottawa sand, it was observed that the consolidation was complete within a minute from the application of the consolidation stress increment. However, a constant time interval of approximately five minutes was allowed before the shear wave velocity was measured across the specimen at this consolidation stress. Then the next stress increment was applied. A similar test procedure was followed for each stress increment until the required consolidation stress or void ratio for triaxial compression loading was achieved. Then the specimens were sheared in triaxial compression under drained or undrained loading conditions. The behavior of the very loose Ottawa sand specimens during drained and undrained loading was presented elsewhere in detail (Sasitharan *et al.*, 1993 and 1994(b)). For specimens deformed to the ultimate critical/steady state, the shear wave velocity at steady state was also measured.

RESULTS AND INTERPRETATION

The consolidation stress, void ratio and shear wave velocity for all of the tests are summarized in Table 1. Figure 2 shows the shear wave velocity and void ratio change during isotropic consolidation for all of the test results for Ottawa sand. From Table 1 and Figure 2 it may be observed that the shear wave velocity changes with consolidation stress and void ratio. The shear wave velocity can be related to void ratio and effective confining stresses using equation 2.

For Ottawa sand, based on the results of this study, the relationship between shear wave velocity (V_S), void ratio (e) and mean effective stress during consolidation (p_c') can be expressed as:

$$V_S = (381 - 259e)\left(\frac{p_c'}{P_a}\right)^{0.26} \text{ m/s} \qquad (6)$$

The material constants 381 and 259 are in units of m/s and P_a is atmospheric pressure (typically P_a = 100 kPa). The stress exponent 0.26 was found to give the best fit to the data for Ottawa sand. This exponent is similar to that suggested by Hardin and Richart (1963) in equation (2). Figure 2b includes contours of constant void ratio using equation 6.

In order to compare the three independent measurements (V_S, e, p_c') the shear wave velocity values can be normalized with respect to the mean effective consolidation stress using a modified form of equation (4), as follows:

$$V_{S1} = V_S \left(\frac{P_a}{p_c'}\right)^n \qquad (7)$$

where n = 0.26 for Ottawa sand.

Figure 3 shows the measured normalized shear wave velocity values as a function of void ratio during consolidation. Hence, based on the test results, the following relationship is valid for Ottawa sand:

$$V_{s1} = (381 - 259e) \text{ m/s} \quad (8)$$

Upper and lower bounds are also shown in Figure 3 to define the extent of scatter in the relationship. These bounds will be used later to define possible limits for the relationship.

Equation (8) was used to fit all of the data over a wide range of void ratio and sample preparation techniques. Figure 4 shows selected typical data in the form of a consolidation plot in terms of e versus log p'. Contours of V_S have been included based on equation (6). Adjacent to each data point is the measured value of V_S for comparison with the derived contours. In general, good agreement is seen between measured and derived V_S values. In another form, a comparison between measured V_S and predicted V_S from equation (6) is shown in Figure 5.

After consolidation, samples were sheared to failure in triaxial compression under either drained or undrained conditions. Samples were sheared to large strains until an ultimate or steady state condition was achieved. At this ultimate steady state (USS), the shear wave velocity was again measured.

Figure 6 shows the ultimate steady states for all of the tests in the form of e versus log p'_{ss} and shear stress (q'_{ss}) versus p'_{ss}. At steady state, the relationship between void ratio, mean normal stress and shear stress can be approximated by:

$$e_{ss} = \Gamma - \lambda \log p'_{ss} \quad (9)$$

$$q_{ss} = M p'_{ss} \quad (10)$$

where: Γ = intercept at 1 kPa;

λ = slope of USSL in e - log p' plane;

M = slope of USSL in q - p' plane.

Based on the tests on Ottawa sand, the parameters that define the ultimate steady state line (USSL) are:

Γ = 0.926

λ = 0.0745

M = 1.2 (i.e. $\phi'_{cv} = 30°$)

These values are valid over an effective stress range of 10 kPa < p' < 800 kPa. Detailed results of the shear testing are given by Sasitharan (1994) and Cunning (1994). Figure 7 shows the normalized stress paths for typical tests in the form of q'/p'_{ss} versus p'/p'_{ss}. This figure clearly shows that samples loose of the USSL (i.e. $p'/p'_{ss} > 1.0$) are contractant and show a strain softening response in undrained shear. Samples dense of the USSL (i.e. $p'/p'_{ss} < 1.0$) are dilatant and show a strain hardening response in undrained shear.

Since V_S measurements were also made at USS, a comparison can be made between USS values and those made during isotropic consolidation using equation (8). Figure 8 shows the normalized shear wave velocity (V_{S1}) versus void ratio (e) at ultimate steady state compared with the consolidation values given by equation (8). The USS values were normalized with respect to the individual stress states based on equation (2):

$$V_{S1} = V_S \left(\frac{P_a}{\sigma_1'}\right)^{n/2} \left(\frac{P_a}{\sigma_3'}\right)^{n/2} \qquad (11)$$

Figure 8 shows that the USS data appear to plot close to the best fit line for Ottawa sand during consolidation. However, the data exist over a small range of void ratio. Figure 8 indicates that the relationship between Vs, e and p' appears to fit consolidation

states as well as ultimate steady states. This suggests that fabric plays a minor role in this relationship for Ottawa sand since the samples during consolidation were prepared using both moist tamping and water pluviation techniques.

EVALUATION OF IN-SITU STATE

The influence of void ratio and stress level on sand behavior is uniquely related to the critical/steady state by the state parameter (Been and Jefferies 1985). Negative and positive state parameter would mean strain hardening and strain softening undrained responses, respectively. The specimens of Ottawa sand consolidated to a void ratio above the steady state line showed a contractant strain softening behavior at large strains during monotonic undrained triaxial compression loading. Samples consolidated to a void ratio below the steady state line showed a dilatant strain hardening response at large strain during undrained triaxial compression loading. Been and Jefferies (1985) defined the state parameter ψ as the void ratio difference between the current state and steady state at the same stress level.

$$\text{i.e.,} \quad \psi = e - e_{ss.} \tag{12}$$

Current void ratio 'e' can be written as (rearranging equation 2):

$$e = \frac{A}{B} - \frac{V_s(P_a)^{na+nb}}{B\,(\sigma'_a)^{na}\,(\sigma'_p)^{nb}} \tag{13}$$

substituting equations 9 and (13) in (12) gives;

$$\psi = \left(\frac{A}{B} - \Gamma\right) - \left(\frac{V_s(P_a)^{na+nb}}{B\,(\sigma'_a)^{na}\,(\sigma'_p)^{nb}} - \lambda \log p'_{ss}\right) \tag{14}$$

Where A, B, λ and Γ are constants for a given sand. Hence, the term (A/B - Γ) is a constant for a given soil. Been and Jefferies (1985) showed that it was possible to estimate the large strain behavior of a clean sand from state parameter (ψ). Hence, it

should be possible to estimate the large strain behavior of a sand from in-situ shear wave velocity measurements using a relationship such as equation 14.

For Ottawa sand, equation 14 can be used to evaluate state parameter (ψ) using the following constants:

$A = 381$ [m/s]

$B = 259$ [m/s]

$na = 0.13$ [-]

$nb = 0.13$ [-]

$\lambda = 0.0745$ [$1/\ell n(kPa)$]

$\Gamma = 0.926$ [-]

For an assumed value of K_o, it is possible to produce curves of V_s versus vertical effective stress (σ_v') for different values of state parameter (ψ). Figure 9 shows the curves for different ψ based on $K_o = 0.4$. The curves in Figure 9 are controlled by the constants (A, B, na, nb, λ and Γ) in equation 14. Based on the work of Hardin and Drnevich (1972) and Tokimatsu *et al.* (1986), the constants (A, B, na and nb) that control the relationship between V_s, void ratio and the effective confining stresses are not expected to change significantly for most uncemented, unaged silica sands. However, the curves in Figure 9 are somewhat sensitive to variations in the USS parameters (Γ and λ) that define the location of the USSL.

Table 2 presents a summary of ultimate steady state parameters for various sands. For most silica sands with rounded to subrounded grains (i.e. similar to Ottawa sand) the parameters Γ and λ are similar to that for Ottawa sand. Hence, the curves shown in Figure 9 should be applicable to other sands with similar intrinsic grain characteristics.

A value of $\psi = 0$ can be used to define the boundary between a net contractive behavior from a net dilative behaviour. Figure 10 shows the variation of V_S with vertical effective stress for two values of the *in-situ* coefficient of earth pressure at rest ($K_o = 0.4$ and 1.0) for $\psi = 0$. Figure 10 clearly shows the importance of the *in-situ* stress state for the evaluation of the boundary between dilatant and contractant sand. However, for low overburden stresses (i.e. $\sigma_v' < 200$ kPa) the influence of K_o is not large.

Figure 11 shows the range for the $\psi = 0$ boundary curve based on the upper and lower bounds from Figure 3. This range represents a variation in V_S of about $\pm$ 10 m/s at $\sigma_v' = 100$ kPa.

Figure 12 compares the derived boundary ($\psi = 0$) for $K_o = 0.4$ with that suggested by Robertson *et al.* (1992) using equation (3) (i.e. V_{s1} = 140 m/s to 160 m/s). Note that Robertson *et al.* (1992) suggested a generalized normalization with n = 0.25. Figure 12 shows that, in general, the relationship proposed by Robertson *et al.* (1992) agrees very well with the boundary based on this study for Ottawa sand. Note that the normalized value of shear wave velocity (V_{s1}) increases with depth from about 140 m/s at σ_v' = 20 kPa to 160 m/s at σ_v' = 200 kPa. This reflects the relatively flat slope of the USSL in the e - log p' plane for Ottawa sand.

PROPOSED APPLICATION

Ideally, in order to evaluate *in-situ* strength and large strain behavior of sands, it is important to conduct laboratory tests on high quality undisturbed specimens. High quality undisturbed specimens of sand can be obtained using *in-situ* ground freezing. Since the cost of *in-situ* ground freezing is high, the need to obtain high quality undisturbed specimens would depend on the project requirements. However, it is

possible to estimate the large strain behavior of a uniform loose sand deposit using *in-situ* shear wave velocity measurements.

Several methods currently exist to measure *in-situ* shear wave velocity profiles in a cost effective way (Stokoe and Hoar, 1987; Woods, 1987; Robertson *et al.*, 1986; Addo and Robertson, 1992). As an initial screening, the curves shown in Figure 9 can be used to estimate state parameter and hence, the large strain behavior of a clean uncemented, young silica sand. Been and Jefferies (1985) provided charts to estimate parameters such as the peak friction angle for sands based on the state parameter ψ.

For a more detailed evaluation for a given sand, it should be possible to develop a material specific relationship between shear wave velocity, void ratio and effective confining stress based on a small number of isotropic consolidation tests on reconstituted specimens of the sand. The shear wave velocity should be measured throughout the consolidation stage and the resulting relationship should have a form similar to that given in equation 5. Several of the very loose specimens can then be loaded in triaxial compression to ultimate steady state. These tests can be performed drained or undrained to provide the parameters that define the USSL (i.e. Γ and λ). These parameters can then be combined with the constants from equation 5 (A, B and n) to produce the relationship to estimate state parameter (ψ) using equation 13, assuming $na = nb = 0.5\ n$.

Provided that the *in-situ* sand deposit is unaged and uncemented, this approach should provide a reasonable estimation of its *in-situ* state. For aged or cemented sands the relationship based on reconstituted specimens may not be valid, since *in-situ* shear wave velocity can be sensitive to the effects of aging and cementation. However, frequently it is the young, uncemented sand deposits that represent the highest risk for flow liquefaction. Therefore, this approach should be applicable as an initial evaluation of such deposits.

One popular in-situ test to measure shear wave velocity is the Seismic Cone Penetration Test (SCPT) (Robertson *et al.*, 1986). The combined measurement of shear wave velocity and penetration resistance (q_c) from the SCPT can be useful to identify aged or cemented sands.

SUMMARY

An experimental study has been presented for shear wave velocity interpretation of clean Ottawa sand based on steady/critical state concepts. Sand specimens were prepared by water pluviation and moist tamping techniques. Shear wave velocities were measured in these specimens during consolidation. Results presented in this study show that shear wave velocities can be expressed in terms of void ratio and effective confining stresses during consolidation. Undrained and drained triaxial compression loading was performed on these specimens to identify the ultimate steady state line and hence, the large strain response (contractive/dilative). For specimens that reached steady state, the shear wave velocities were also measured at steady state.

Based on the relationship between void ratio, effective confining stress and shear wave velocity plus the equation for the ultimate steady state line, the *in-situ* state of the sand can be estimated. The contractive/dilative behavior can be evaluated from shear wave velocity and the vertical effective stress with an estimate of K_O.

The relationships developed in this study are limited to clean, uncemented, freshly deposited Ottawa sand. For aged or cemented sands, the relationship based on reconstituted specimens may not be valid. However, frequently it is young, uncemented sand deposits that represent the highest risk of flow liquefaction. Further work is required to confirm and clarify the above relationship for other sands including silty sands .

ACKNOWLEDGMENTS

The financial support of the Natural Science and Engineering Research Council of Canada (NSERC) is gratefully acknowledged. The authors would like to acknowledge the valuable assistance of the University of Alberta, Department of Civil Engineering technical staff. G. Cyre provided prompt and valuable support in the design, construction and maintenance of the test apparatus. Many thanks to S. Gamble whose knowledge and availability were so helpful during the experimental work. The authors would also like to acknowledge the useful comments from the reviewers.

REFERENCES

Addo, K. and Robertson, P.K. 1992. Shear wave velocity measurements of soils using Rayleigh waves. Canadian Geotechnical Journal, **29**: 558-568.

Been, K.H. and Jefferies, M.G. 1985. A state parameter for sands. Geotechnique, **35**: 99-112.

Been. K., Jefferies, M.G. and Hachey, J. 1991. The critical state of sand. Geotechnique, **41**: 365-381.

Bierschwale, J.G. and Stokoe, K.H. 1984. Analytical evaluation of liquefaction potential of sand subjected to the 1981 Westmoreland Earthquake. Geotechnical Engineering Report GR-84-15, Civil Engineering Department, University of Texas, Austin, Texas.

Castro, G. 1969. Liquefaction of sands. Harvard Soil Mechanics Series No. 81. 112 pp.

Cunning, J.C., 1994. Shear wave velocity of cohesionless soils for evaluation of *in-situ* state. M.Sc. thesis, Department of Civil Engineering, The University of Alberta, Alberta, Canada.

De Alba, P., Baldwin, K., Janoo, V., Roe, G. and Celikkol, B. 1984. Elastic wave velocities and liquefaction potential. Geotechnical Testing Journal, American Standards for Testing and Materials, **7(2)**: 77-88.

Han, C. and Vardoulakis, I.G. 1991. Plane strain compression experiments on water saturated fine grained sand. Geotechnique, **41**: 49-78.

Hardin, B.O. and Drnevich, V.P., 1972. Shear modulus and damping of soils; measurements and parameter effects, Journal of Soil Mechanics and Foundation Division, American Society of Civil Engineering, **98**(6): 603-624.

Hardin, B.O. and Richart, F.E. Jr. 1963. Elastic wave velocities in granular soils. Journal of the Soil Mechanics and Foundation Engineering, American Society of Civil Engineering, **89**(1): 33-65.

Hatanaka, M., Suginato, M. and Suzudi, Y. 1985. Liquefaction resistance of alluvial volcanic soils specimens by in situ freezing. Soils and Foundations, **25**(3): 49-63.

Ishihara. K. 1993. Liquefaction and flow failure during earthquakes. The 33rd Rankine lecture. Geotechnique **43:** .

Kayen, R.E., Mitchell, J.K., Seed, R.B.B., Lodge, A., Nishio, S. and Coutinho, R. 1992. Evaluation of SPT-, CPT-, and Shear Wave-Based methods for liquefaction potential assessment using Loma Prieta data. US-Japan Workshop. pp. 177-204.

Konrad, J.M. 1990. Sampling of saturated and unsaturated sands by freezing. Geotechnical Testing Journal, American Standards for Testing and Materials, **13**(2): 88-96.

Negussey, D. 1984. An experimental study of small strain response of sand. Ph. D. Thesis, The University of British Columbia, Vancouver, B.C., Canada.

Robertson, P.K. 1993. Design consideration for liquefaction. US-Japan Workshop, June 1993.

Robertson, P.K., Campanella, R.G., Gillespie, D. and Rice, A. 1986. Seismic CPT to measure in-situ shear wave velocity. Journal of Geotechnical Engineering, American Society of Civil Engineering, **112**(8): 791-803.

Robertson, P.K., Woeller, D.J. and Finn, W.D.L. 1992. Seismic cone penetration test for evaluating liquefaction potential under cyclic loading. Canadian Geotechnical Journal, **29**: 686-695.

Roscoe, K.H., Schofield, A.N. and Wroth, C.P. 1958. On yielding of soils. Geotechnique, **8**: 22-53.

Rosler, S.K. 1979. Anisotropic shear wave modulus due to stress anisotropy. Journal of Geotechnical Engineering, American Society of Civil Engineering, **105**(7): 871-880.

Sasitharan, S. 1989. Stress path dependency of dilatancy and stress-strain response of sand. M.A.Sc. Thesis. Department of Civil Engineering, The University of British Columbia, Vancouver, BC., Canada.

Sasitharan, S. 1994. Collapse Behavior of Very Loose Sand. Ph.D. Thesis. Department of Civil Engineering, The University of Alberta, Alberta, Canada.

Sasitharan, S., Robertson, P.K. and Sego, D.C. 1994(a). Sample disturbance from shear wave velocity measurements. Canadian Geotechnical Journal **31:** 119-124.

Sasitharan, S., Robertson, P.K., Sego, D.C. and Morgenstern, N.R. 1994(b). Collapse behavior of sand. Canadian Geotechnical Journal, **30**: 569-577.

Sasitharan, S., Robertson, P.K., Sego, D.C. and Morgenstern, N.R. 1994. A State boundary surface for very loose sand and it's practical applications. Canadian Geotechnical Journal. Accepted for publication.

Seed, H.B., Idriss, I.M. and Arango, I. 1983. Evaluation of liquefaction potential using field performance data. Journal of Geotechnical Engineering, American Society of Civil Engineering, **109**(3): 458-482.

Sego, D.C., Robertson, P.K , Sasitharan, S., Kilpatrick, B.I. and Pillai, V.S. 1993. Ground freezing and sampling of foundation soils at Duncan Dam. 46th Canadian Geotechnical Conference, Saskatoon. pp. 237-246.

Shirley, E.T. 1978. An improved shear wave transducer. Journal of Acoustical Society of America, **63**: 1643-1645.

Sladen, J.A., and Hewitt, K.J. 1989. Influence of placement method of the in-situ density of hydraulic fills. Canadian Geotechnical Journal, **26**: 453-466.

Stokoe, K.H. II., Lee, H.H.S. and Knox. D.P. 1985. Shear moduli measurements under true triaxial stresses. Proceedings, Advances in the art of testing soils under cyclic conditions, American Society of Civil Engineers, Detroit, MI, pp. 166-185.

Stokoe, K.H. II. and Hoar, R.J. 1987. Variables affecting in-situ seismic measurements. Proceedings, Conference on Earthquake Engineering and Soil Dynamics, American Society of Civil Engineers, Vol. II. pp. 919-939.

Tokimatsu, K., Yanazaki, T. and Yoshimi, Y. 1986. Soil liquefaction evaluation by elastic shear moduli, Soils and Foundations, **26**(1): 25-35.

Tokimatsu, K. and Uchida, A. 1990. Correlation between liquefaction resistance and shear wave velocity. Soils and Foundations, **30**(2): 33-42.

Woods, R.D. 1987. In-situ tests for foundation vibrations. Proceedings, Conference on use of in-situ tests in geotechnical engineering, American Society of Civil Engineers, Special Publication 6, pp. 336-375.

Yoshimi, Y. Tokimatsu, K., Kaneko, O. and Makihara, Y., 1984. Undrained cyclic shear strength of a dense Niigata sand. Soils and Foundations, **24**(4):131-145.

Yoshimi, Y. Tokimatsu, K. and Hosaka, Y., 1989. Evaluation of liquefaction resistance of clean sands based on high quality undisturbed specimens. Soils and Foundations, **29**(1):93-104.

Yu, P. and Richard, F.E. Jr. 1984. Stress ratio effect on shear modulus of dry sands. Journal of Geotechnical Engineering, American Society of Civil Engineering, **110**(3): 331-341.

NOTATION

The following symbols are used in this paper

e = void ratio;

P_a = the reference pressure (usually 100 kPa);

p' = the effective mean normal stress;

p'_c = the effective mean normal stress during consolidation;

A = constant;

B = constant.

na = constant;

nb = constant;

m_1 = constant;

m_2 = constant;

V_S = the shear wave velocity.;

V_{S1} = the normalized shear wave velocity;

σ'_a = the effective stress in the direction of wave propagation;

σ'_p = the effective stress in the direction of particle motion;

σ'_v = the effective overburden pressure;

Γ = the intercept of the steady state line at $p'_{SS} = 1$;

λ = slope of the steady state line in e-log p' space;

ψ = state parameter

List of tables

List of Figures

Fig. (12) Comparison of proposed profile for $\psi = 0$ for Ottawa sand with $K_o = 0.4$ with range suggested by Robertson *et al.* (1992).

Preparation	p'c, (kPa)	e	Vs, (m/s)
MT	100.6	0.814	175
	151.8	0.809	192
	200.8	0.805	212
	250.7	0.802	226
	300.4	0.799	234
	350.5	0.796	245
	400.2	0.794	253
	442.9	0.792	258
	500.7	0.791	267
MT	150.3	0.827	189
	250.7	0.819	207
	350.5	0.813	223
	450.9	0.809	246
	550.6	0.806	258
MT	148.9	0.824	200
	248.9	0.817	228
	349.4	0.812	249
MT	151.2	0.822	202
	254.9	0.816	227
MT	49.1	0.822	138
	148.2	0.813	184
	247.3	0.807	207
	348.8	0.803	224
MT	52.6	0.826	139
	147.7	0.816	184
	247.6	0.808	208
	346.1	0.804	227

Preparation	p'c, (kPa)	e	Vs, (m/s)
MT	45.5	0.875	122
	144.3	0.871	174
	239.4	0.865	198
	336.3	0.858	231
MT	153.7	0.894	181
MT	59.0	0.895	123
	258.0	0.859	221
MT	66.0	0.802	161
	161.0	0.789	200
	261.0	0.775	237
MT	163.0	0.801	201
	261.0	0.793	210
	363.0	0.784	256
MT	63.0	0.770	149
	154.0	0.762	193
	252.0	0.754	225
	351.0	0.749	251

Preparation	p'c, (kPa)	e	Vs, (m/s)
WP	52.9	0.666	183
	76.5	0.663	198
	102.1	0.661	221
WP	102.1	0.682	210
	152.4	0.678	236
	202.6	0.675	255
	253.7	0.672	278
	302.7	0.671	293
	354	0.669	306
	404	0.667	308
WP	58.8	0.679	181
	108.3	0.674	222
WP	107.2	0.675	212
	157.2	0.671	226
	207.5	0.667	265
	257.3	0.665	278
	307.8	0.663	282
	407.9	0.659	308

Preparation	p'c, (kPa)	e	Vs, (m/s)
WP	55	0.584	181
	105	0.580	235
	156.5	0.578	261
	207.3	0.575	284
	257.2	0.573	300
	306.6	0.570	320
	357.5	0.569	324
	405.1	0.568	333
WP	57.5	0.585	198
	107.1	0.582	231
	173.5	0.578	248
	207.4	0.577	278
	256.7	0.575	299
	307.7	0.574	322
	358.6	0.572	328
	419.1	0.571	336

Table 1 Summary of shear wave velocity measurements during consolidation.

Sand	Source	Mineralogy	emax	emin	Gs	M	s		λ	Γ	
							State boundary	Collapse surface			
Ottawa (C109)	present study	quartz (rounded to subrounded)	0.820	0.500	2.66	1.19	0.80	0.51	0.0168	0.864	
Erksak	Been et al (1991)	73 % quartz 22 % feldspar (rounded to subrounded)	0.753	0.527	2.66	1.24	0.97	0.70	0.0133 0.1346	0.820 1.167	p'ss < 1000 kPa p'ss > 1000 kPa
Toyoura	Ishihara (1992) and Tokimatsu et al (1986)	75 % quartz 25 % feldspar (rounded to subrounded)	0.973	0.635	2.64	1.24	0.93	0.58	0.0043 0.0283 0.1210	0.938 1.048 1.677	p'ss < 100 kPa 100 kPa < p'ss < 1000 kPa p'ss > 1100 kPa
Lornex	Castro et al (1982)	quartz (angular)	1.080	0.680	2.68	1.42	1.36	0.83	0.0220 0.1470	1.100 1.762	p'ss < 200 kPa p'ss > 200 kPa
Brenda	Klohn Leonoff Report (January 18, 1984)	85 % quartz 15 % mica	1.060	0.688	2.70	1.46	1.17	0.73	0.0420 0.1087	1.112 1.492	p'ss < 200 kPa p'ss > 200 kPa
Syncrude	Sladen and Hanford (1987)	95 % quartz	0.930	0.550	_	1.19	0.64	0.50	0.0170	0.847	
Nerlerk	Sladen et al (1985)	_	0.890	0.660	_	1.20	0.89	0.62	0.0145	0.885	
Leight Buzzar	Sladen et al (1985)	quartz	0.750	0.580	_	1.19	0.73	0.54	0.0347	1.000	

Table (2)

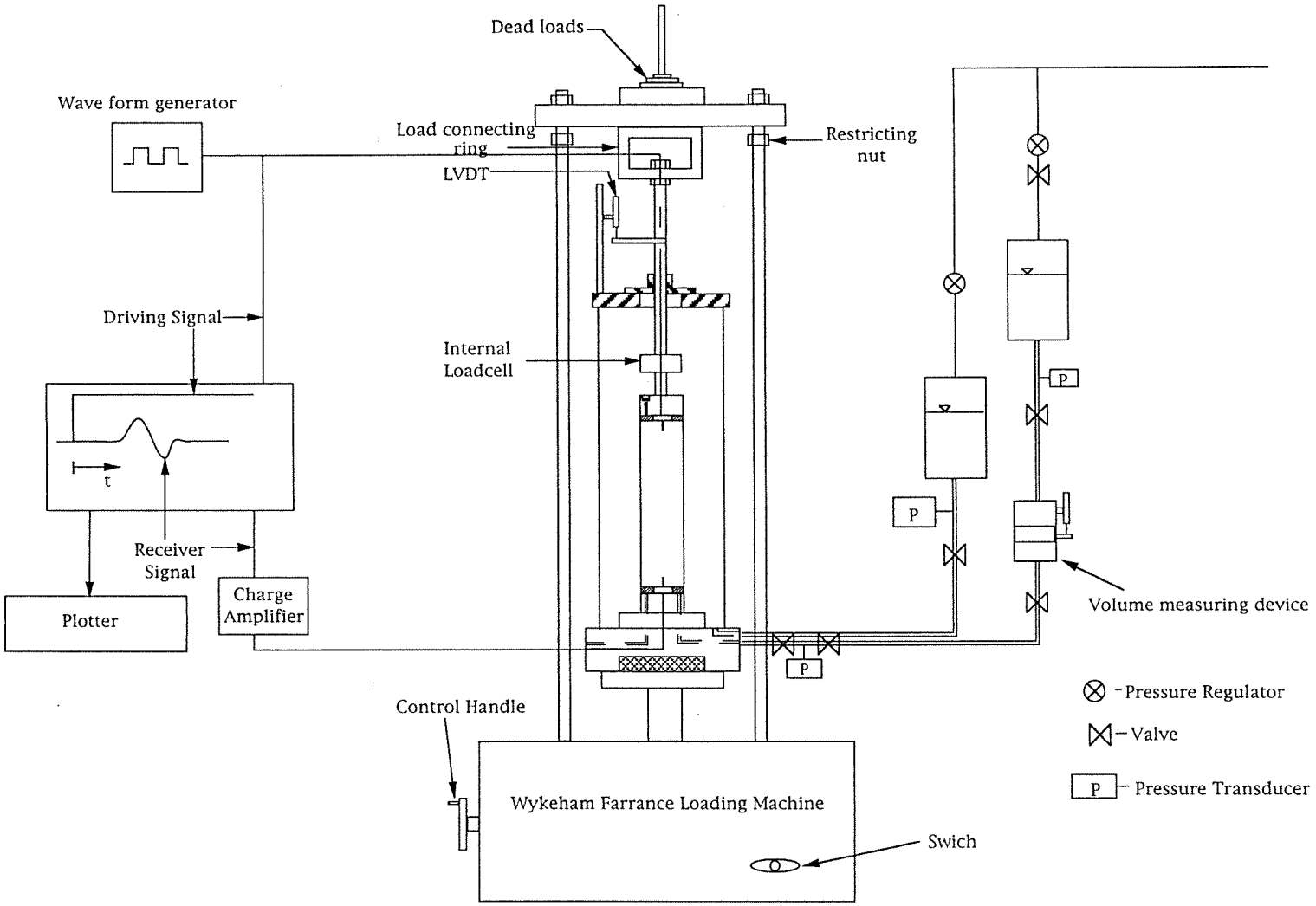
Dead loads
Wave form generator
Load connecting ring
LVDT
Restricting nut
Driving Signal
Internal Loadcell
t
Receiver Signal
Plotter
Charge Amplifier
P
Volume measuring device
Control Handle
Wykeham Farrance Loading Machine
Swich
Pressure Regulator
Valve
Pressure Transducer

Fig (1)

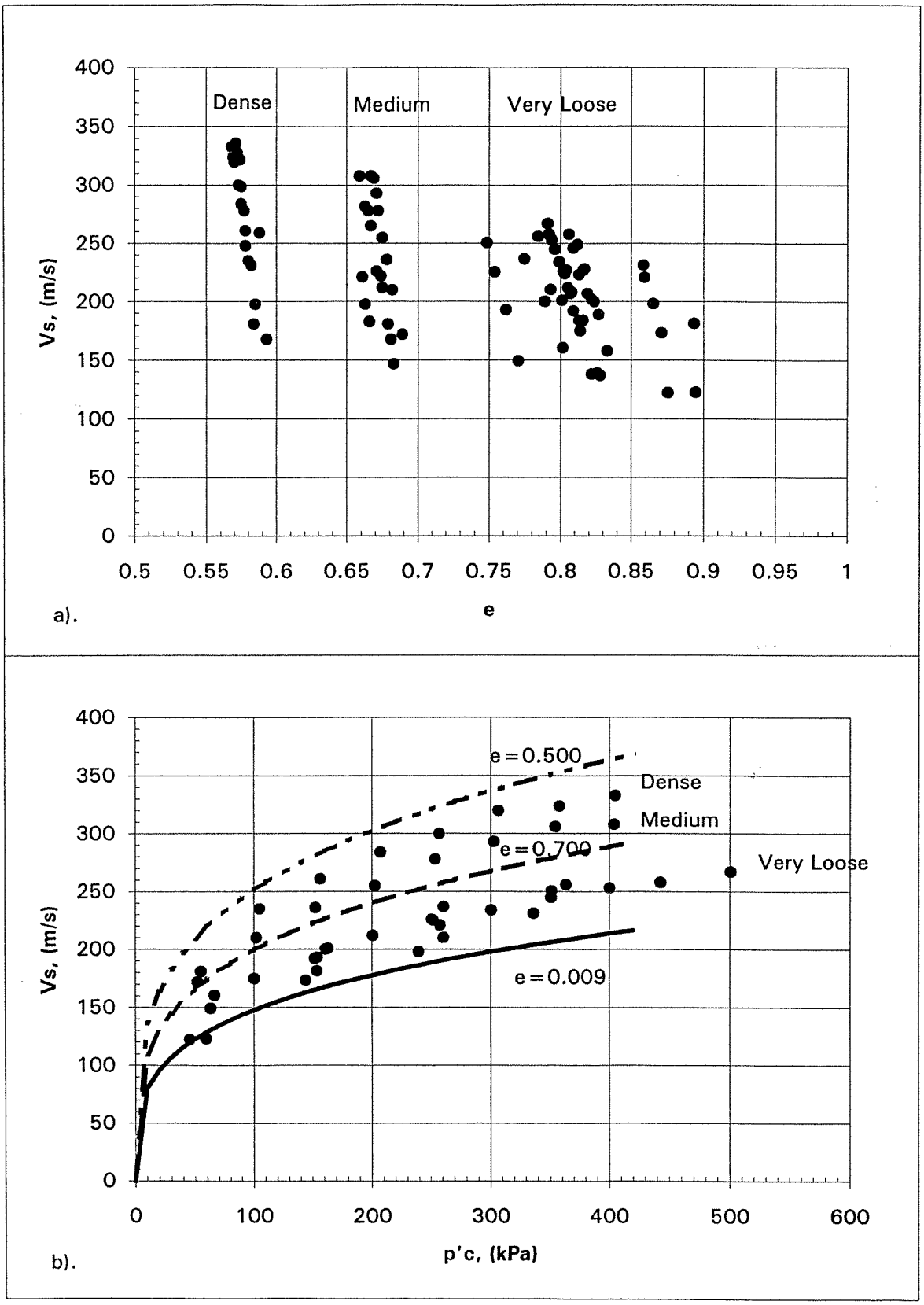
Dense
Medium
Very Loose
Vs, (m/s)
e
a).
e = 0.500
e = 0.700
e = 0.009
Dense
Medium
Very Loose
Vs, (m/s)
p'c, (kPa)
b).

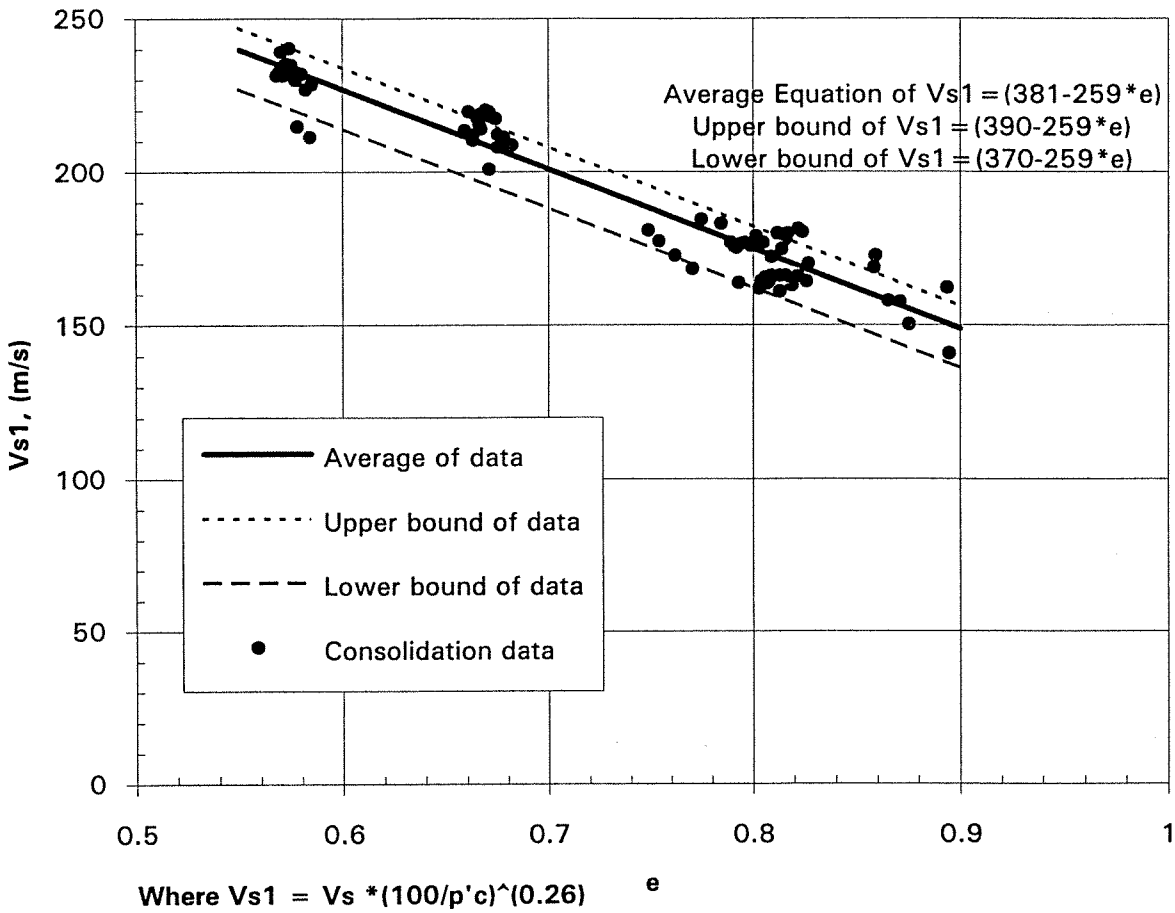
Average Equation of Vs1 = (381-259*e)
Upper bound of Vs1 = (390-259*e)
Lower bound of Vs1 = (370-259*e)
Average of data
Upper bound of data
Lower bound of data
Consolidation data
Vs1, (m/s)
250
200
150
100
50
0
0.5
0.6
0.7
0.8
0.9
1
e
Where Vs1 = Vs *(100/p'c)^(0.26)

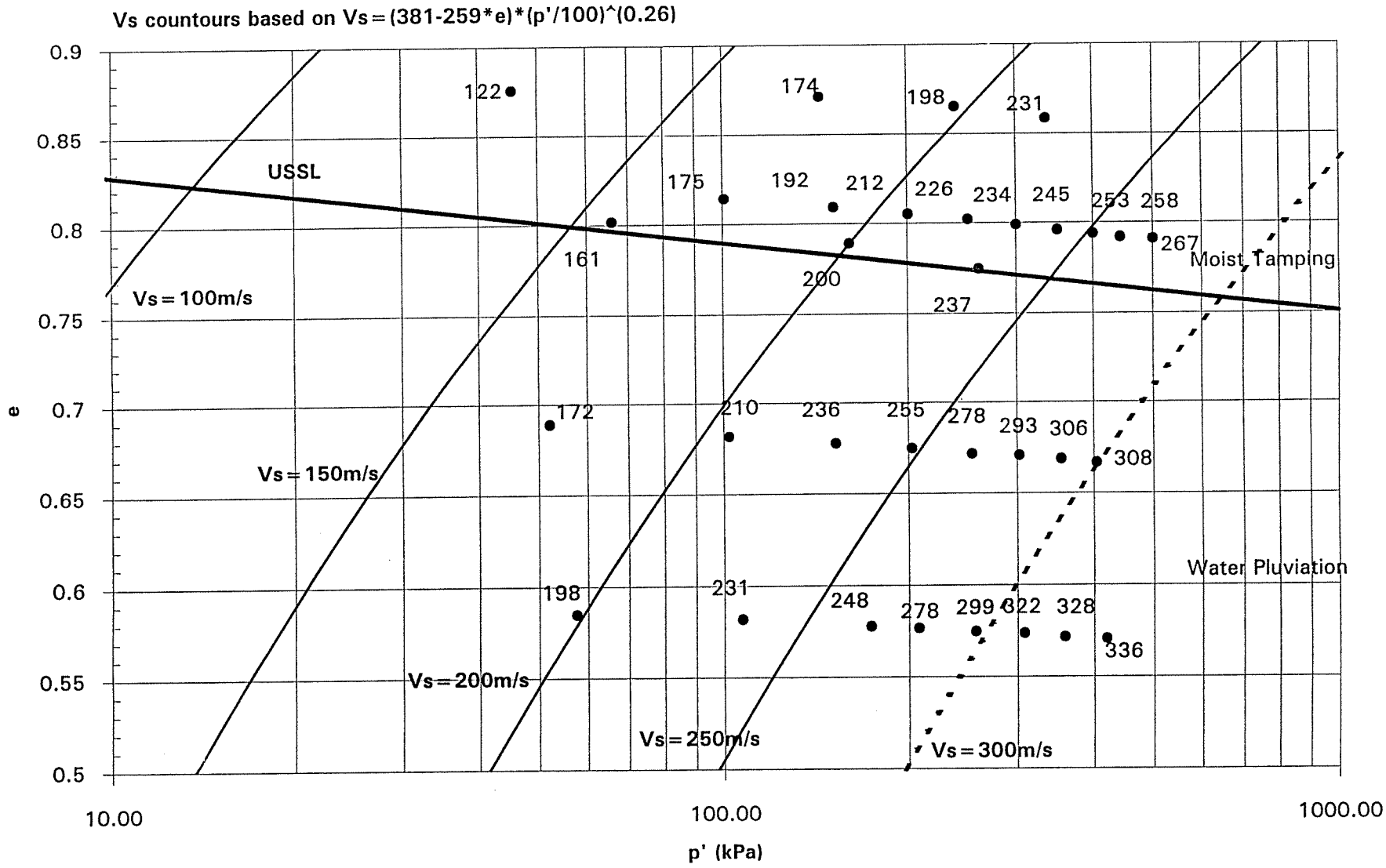
Vs countours based on Vs=(381-259*e)*(p'/100)^(0.26)
0.9
0.85
0.8
0.75
0.7
0.65
0.6
0.55
0.5
e
10.00
100.00
1000.00
p' (kPa)
USSL
Vs=100m/s
Vs=150m/s
Vs=200m/s
Vs=250m/s
Vs=300m/s
Moist Tamping
Water Pluviation
122
174
198
231
175
192
212
226
234
245
253
258
267
161
200
237
172
210
236
255
278
293
306
308
198
231
248
278
299
322
328
336

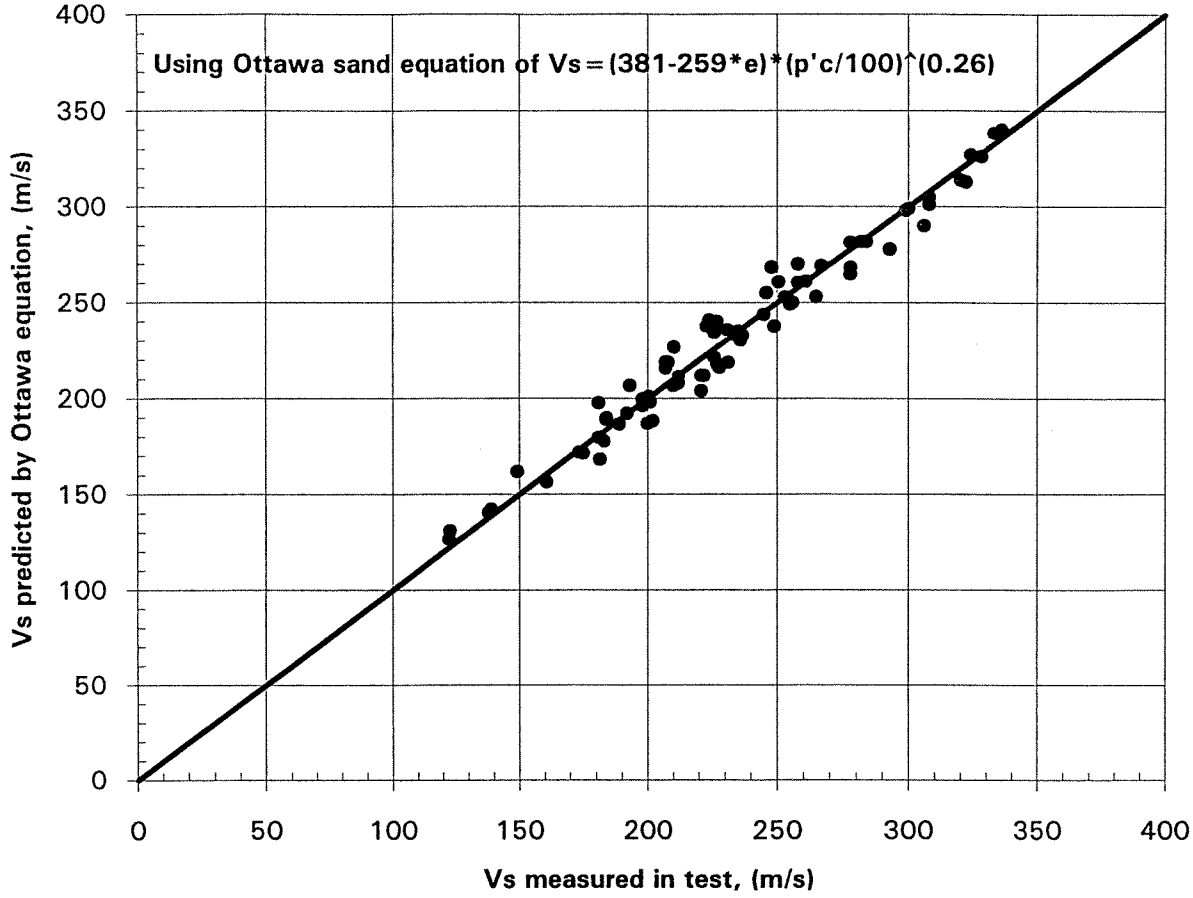
Using Ottawa sand equation of Vs = (381-259*e)*(p'c/100)^(0.26)
Vs predicted by Ottawa equation, (m/s)
Vs measured in test, (m/s)
0
50
100
150
200
250
300
350
400

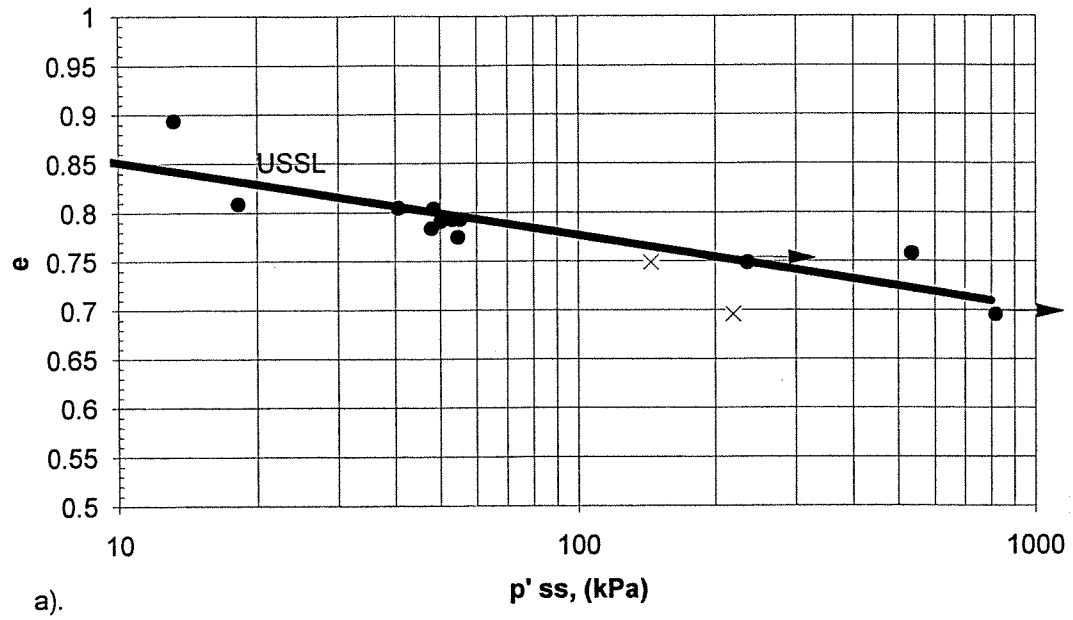

a).

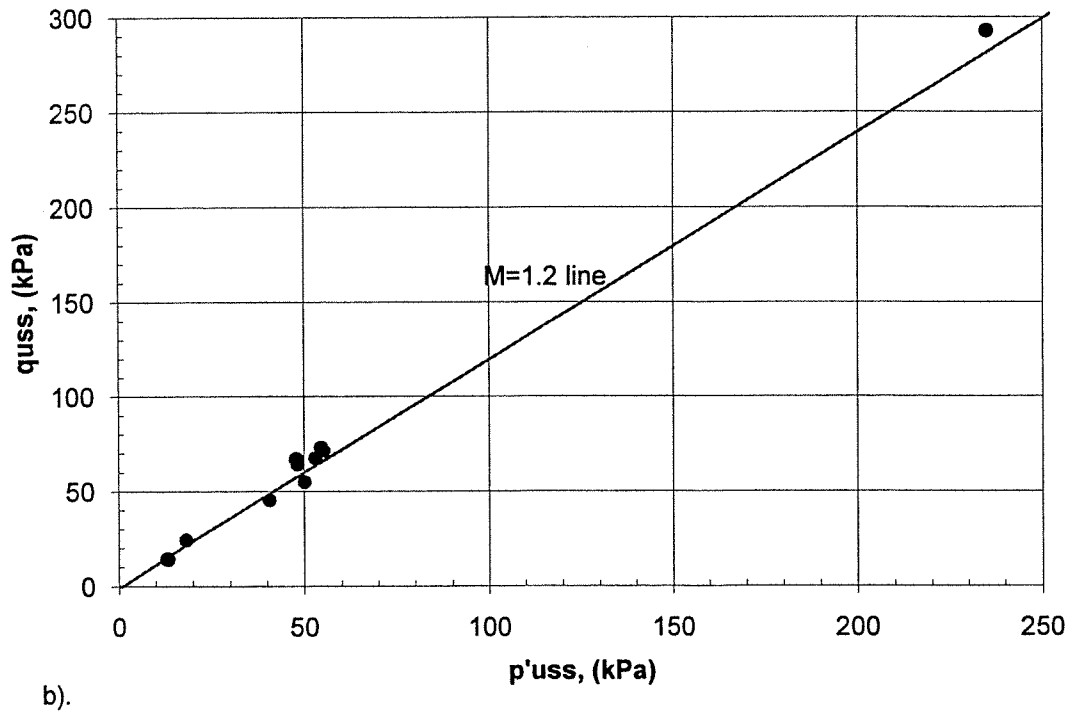

b).

USS Parameters $\Gamma = 0.926$, $\lambda = 0.0745$, $M = 1.2 (\phi cv = 30°)$

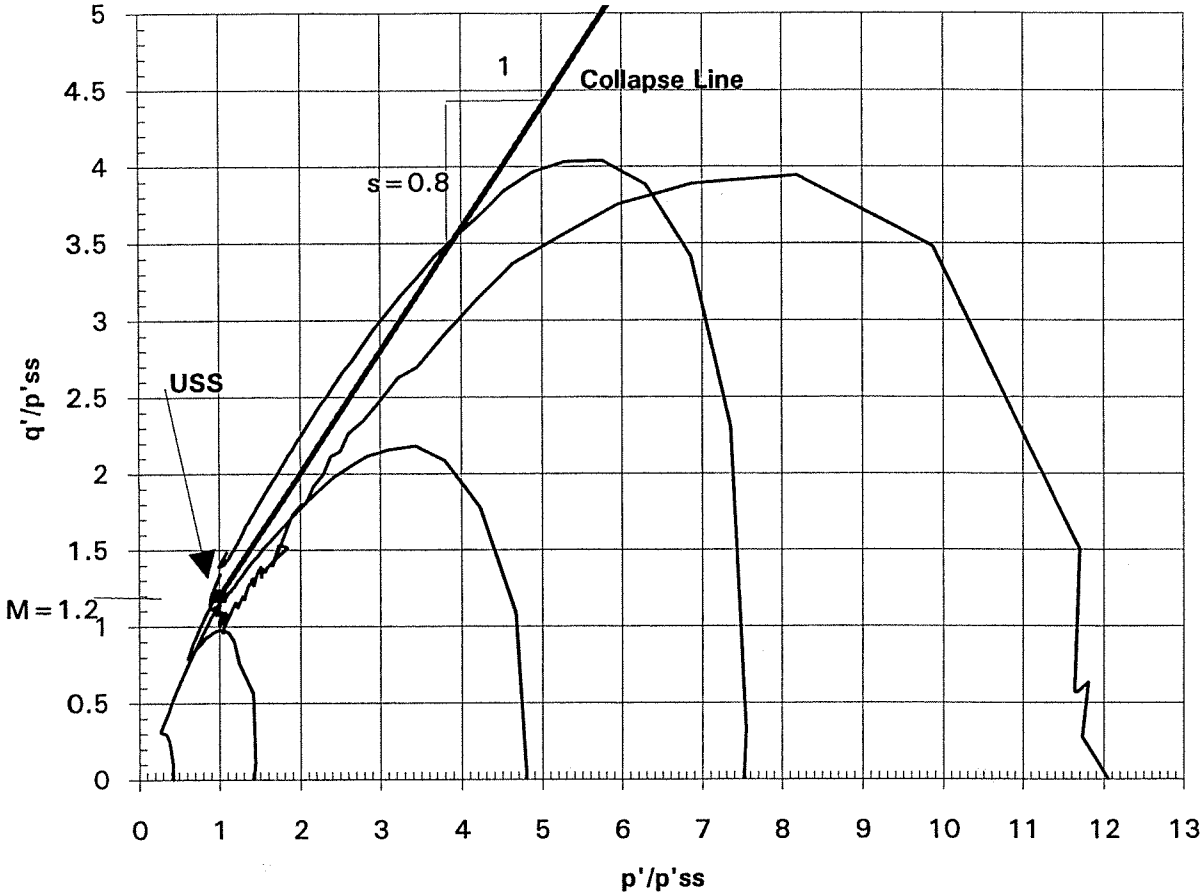
5
4.5
4
3.5
3
2.5
2
1.5
1
0.5
0
0
1
2
3
4
5
6
7
8
9
10
11
12
13
q'/p'ss
p'/p'ss
1
Collapse Line
s=0.8
USS
M=1.2

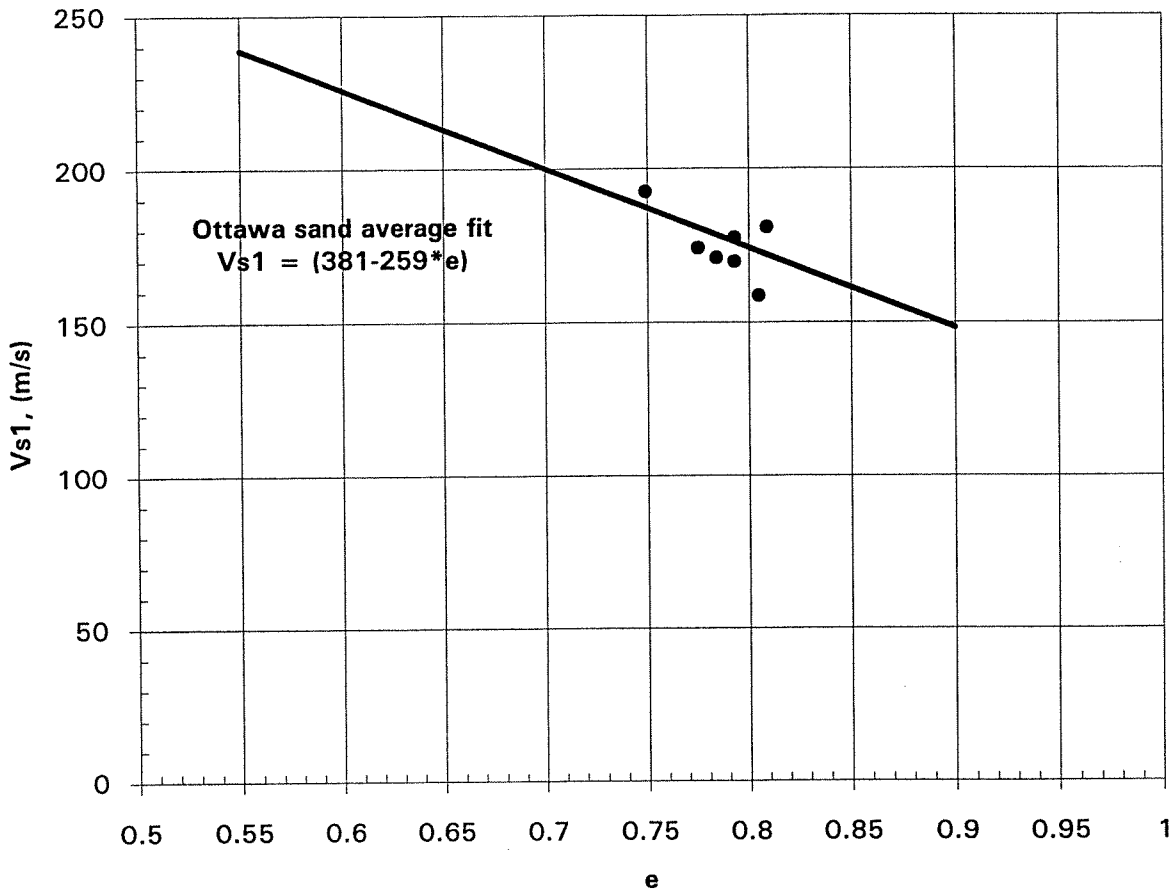
Ottawa sand average fit
Vs1 = (381-259*e)
Vs1, (m/s)
250
200
150
100
50
0
0.5
0.55
0.6
0.65
0.7
0.75
0.8
0.85
0.9
0.95
1
e

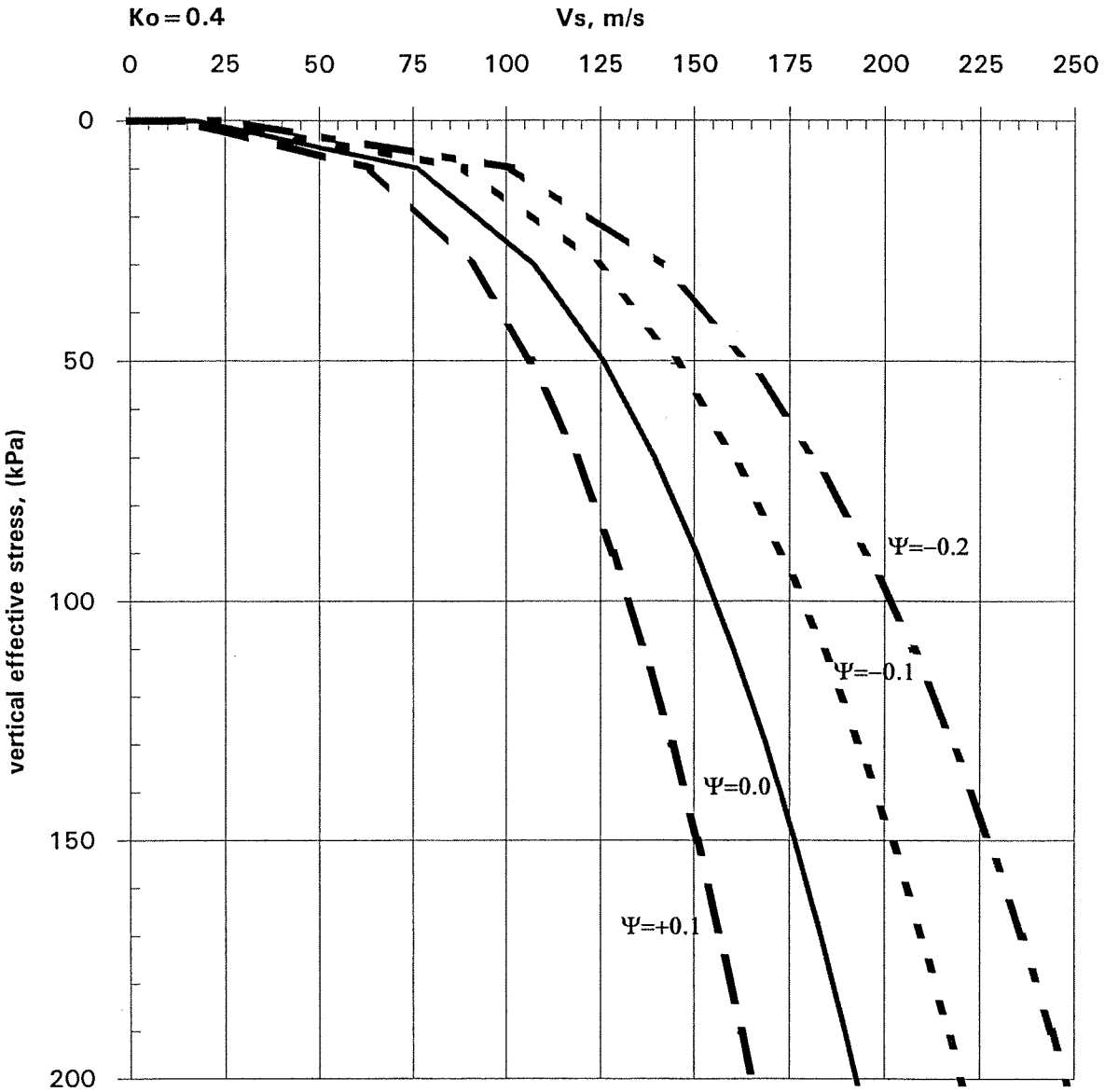
Ko = 0.4
Vs, m/s
0
25
50
75
100
125
150
175
200
225
250
0
50
100
150
200
vertical effective stress, (kPa)
Ψ=–0.2
Ψ=–0.1
Ψ=0.0
Ψ=+0.1

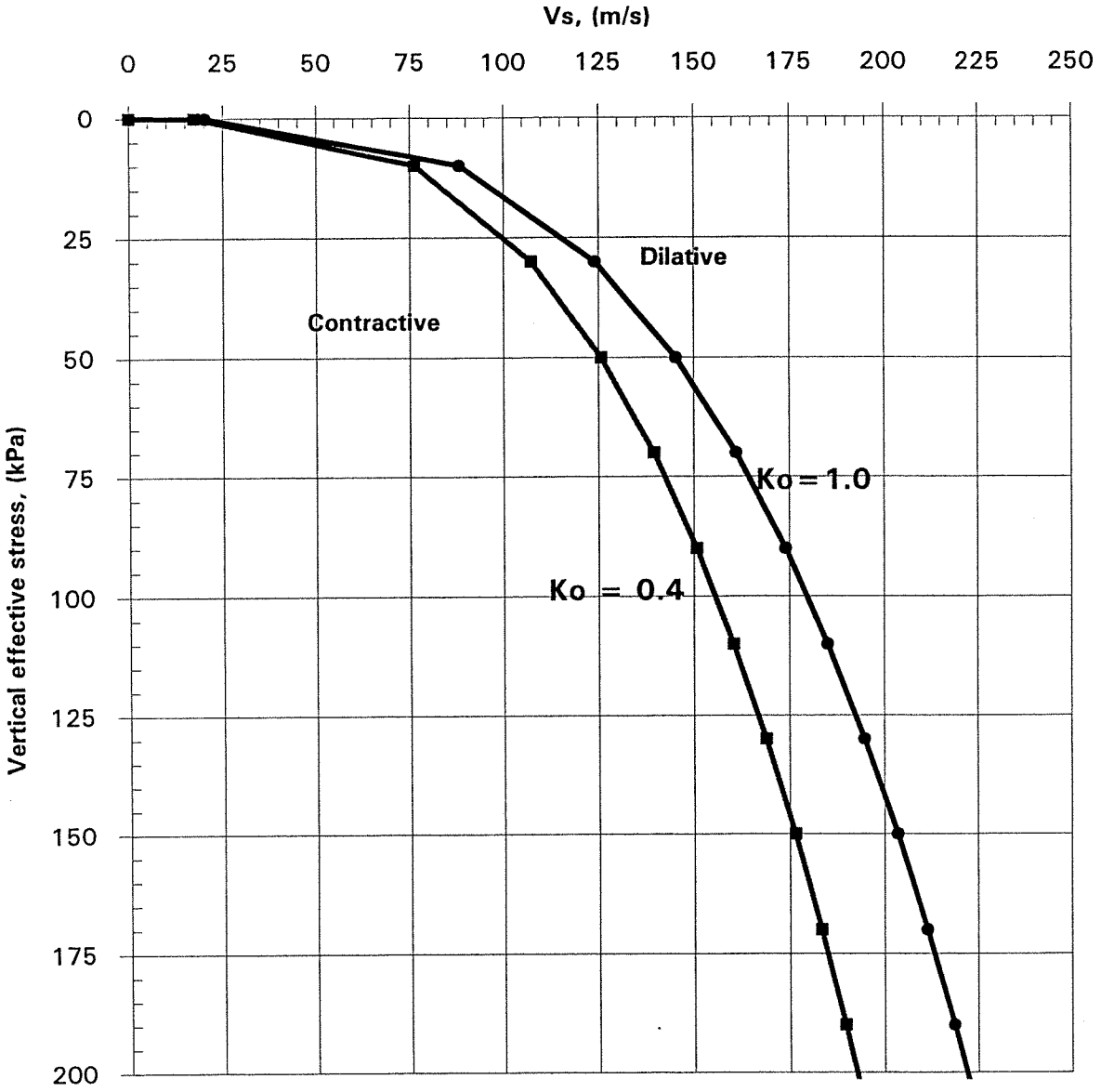
Vs, (m/s)
0
25
50
75
100
125
150
175
200
225
250
Vertical effective stress, (kPa)
0
25
50
75
100
125
150
175
200
Dilative
Contractive
Ko = 1.0
Ko = 0.4

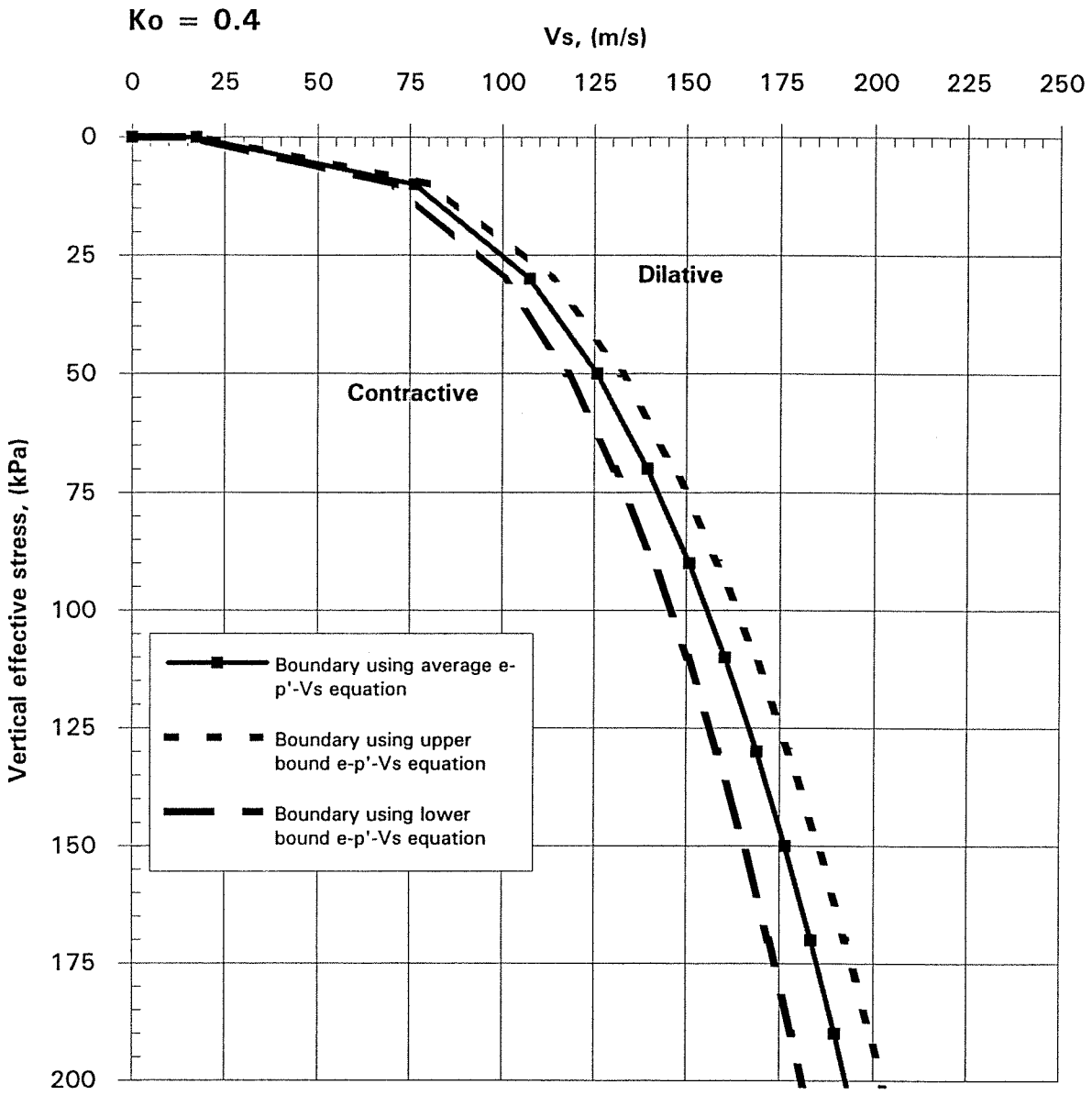
Ko = 0.4
Vs, (m/s)
0
25
50
75
100
125
150
175
200
225
250
Vertical effective stress, (kPa)
Dilative
Contractive
Boundary using average e-p'-Vs equation
Boundary using upper bound e-p'-Vs equation
Boundary using lower bound e-p'-Vs equation

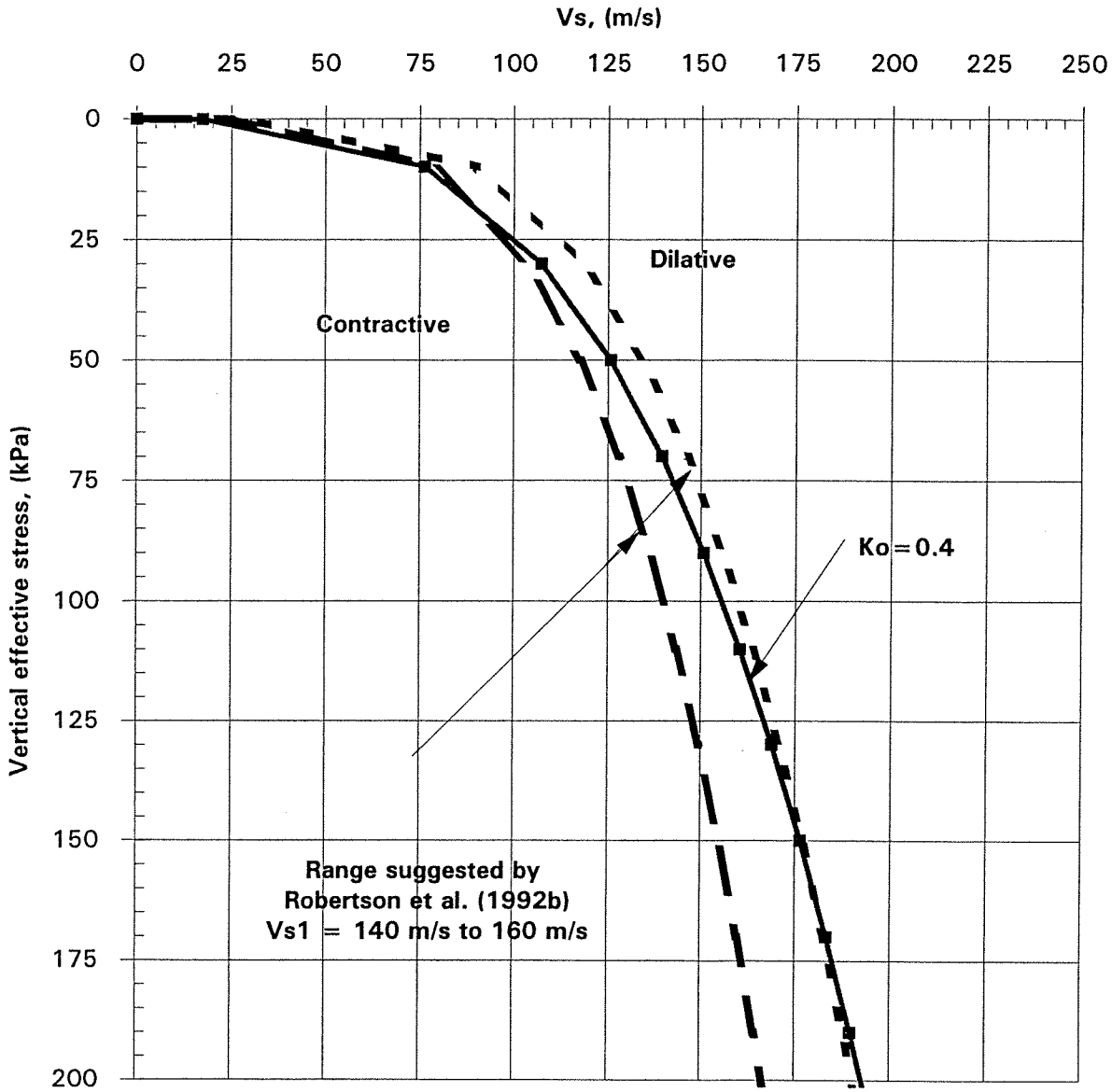
Vs, (m/s)
0
25
50
75
100
125
150
175
200
225
250
Vertical effective stress, (kPa)
0
25
50
75
100
125
150
175
200
Dilative
Contractive
Ko = 0.4
Range suggested by
Robertson et al. (1992b)
Vs1 = 140 m/s to 160 m/s